Tapered multi-mode interference couplers for high order mode power extraction

2010 J. Opt. 12 075502

(http://iopscience.iop.org/2040-8986/12/7/075502)

J. Opt. **12** (2010) 075502 (5pp) doi:10.1088/2040-8978/12/7/075502

Tapered multi-mode interference couplers for high order mode power extraction

Amir Hosseini, John Covey, David N Kwong and Ray T Chen

Microelectronics Research Center, Electrical and Computer Engineering Department, University of Texas at Austin, Austin, TX 78758, USA

E-mail: ahoss@mail.utexas.edu and raychen@uts.cc.utexas.edu

Received 6 April 2010, accepted for publication 27 May 2010
Published 23 June 2010
Online at stacks.iop.org/JOpt/12/075502

Abstract
Tapered 1 × 1 multi-mode interference (MMI) devices are proposed for high order to fundamental mode conversion. Like adiabatic tapers, the device provides a down-tapered image of the input fundamental mode, while acting as a short taper for higher even-ordered modes. This is the first tapering scheme capable of near 100% transmission of the input fundamental mode, as well as mode conversion for the input higher order modes. When directly excited by diode lasers, the tapered MMI coupler presented can convert the fundamental and second-order transverse modes of different wavelengths into the fundamental mode signals of a single-mode output waveguide.

Keywords: multimode interference couplers, waveguide theory, self-imaging in optical waveguides

(Some figures in this article are in colour only in the electronic version)

1. Introduction

Accommodating various sizes, shapes, and modes of guided light is essential for flexibility in photonic integrated circuit (PIC) design. Specifically, spot size and waveguide mode order conversion can allow PICs to utilize a wide range of laser sources as well as many waveguide geometries. Tapered structures are commonly used to perform the necessary profile shaping.

In adiabatic tapers the waveguide width changes so slowly that the mode conversion is negligible [1, 2]. Therefore, if the taper output is a single-mode (SM) waveguide, the power in the input fundamental is perfectly transmitted into the output waveguide, while all the input power in the high order modes is radiated away.

For short tapers, mode conversion has a vital role. Despite the advantage of shorter lengths, such tapers suffer from severe tolerance control of the structure's geometry and refractive indices. One can define a modal transmission coefficient: $A_{m0} = |\int_S \varphi_{0,\mathrm{out}}\varphi^*_{m,\mathrm{in}}\,\mathrm{d}x\,\mathrm{d}y|$, where the normalized mth-order mode ($\varphi_{m,\mathrm{in}}$) of the input waveguide excites the fundamental mode in the output waveguide ($\varphi_{0,\mathrm{out}}$) [2]. For the SM output waveguide, short or abrupt tapers can result in non-zero A_{m0} coefficients for any integer $m > 1$. However, the mismatch between the fields of the fundamental modes in the input and output significantly lowers A_{00}. Also note that on the basis of the definition of perfect adiabatic tapering, when a multi-mode (MM) waveguide is adiabatically tapered down to an SM waveguide, we have $A_{00} = 1$, while all $A_{m0} = 1$ for any integer value $m > 1$.

Our goal is to use tapered 1 × 1 MMIs with an MM input and an SM output in order to extract and convert power from the high order modes in the input to the SM output without jeopardizing the transmission efficiency of the input fundamental mode (A_{00}). Instead of directly converting MM to SM, most MMI designs act as $M \times N$ switches, splitters, or multiplexers [4–6]. To our knowledge, utilizing an MMI to interface MM inputs with SM outputs has not been investigated.

2. 1 × 1 tapered MMI design

For a straight MMI device, the single image of the input field distribution repeats itself every $3L_\pi$, where $L_\pi = 4n_{\mathrm{eff}}W_{\mathrm{e}}^2/3\lambda_0$, n_{eff} is the effective refractive index of the MM waveguide, W_{e} is the effective MMI width, which includes the geometric width of MMI and mode penetration into the

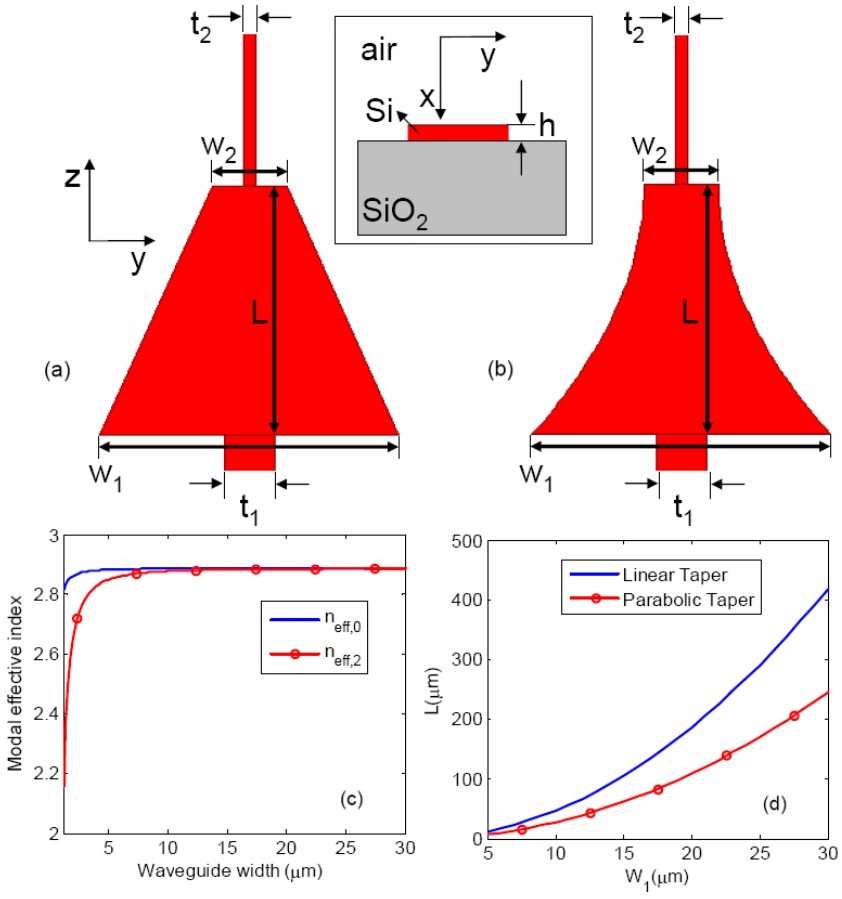

Figure 1. ((a), (b)) Schematics of linear and parabolic tapering. Inset shows a cross-section view of the waveguide structure. (c) Effective indices of the zeroth-order and the second-order TE polarized modes versus waveguide width for a waveguide thickness of 0.25 μm, $n_{\mathrm{Si}} = 3.47$, $n_{\mathrm{SiO_2}} = 1.45$. (d) Variations of MMI length versus the input MMI width (W_1) for the output/input width ratio being $w_2/w_1 = 1/4$ for linear and parabolic tapering types.

cladding layers, and λ_0 is the wavelength in vacuum. When the MMI input is restricted to symmetric excitation, the required device length becomes four times shorter ($3L_\pi/4$). Since MMI length is proportional to the square of the MMI width, tapered MMIs have been utilized to reduce device length by a factor of 3–4 [3, 4]. Recently, compact 2×2 parabolically tapered MMI couplers were theoretically and experimentally investigated [4, 5, 7]. When the MMI width is tapered down with respect to its width at the input, we notice that the output image is also reduced in width. The overall transmission can approach 100% provided that (1) the taper structure is adiabatic, (2) the excited high order modes at the input of the MM waveguide are supported by the width of the MM waveguide at the output. The question to be answered is what happens to the high order input modes when the output waveguide is SM (see figures 1(a) and (b)). Although all input field profiles decompose into the modal field distributions of the MM waveguide, the field excitation components of the high order modes are stronger in the case of high order mode inputs compared to the fundamental mode input case [7].

Since high order modes in the MM waveguide are more likely to be radiated out of the waveguide at the narrowed region, we expect lower transmission for these modes. Additionally, since the number of modes supported by the MM waveguide at the output can be fewer than for the input, the image resolution at the output can be too coarse to resolve the field variation of the input high order modes. Thus, a low resolution image of a high order mode input can excite the SM output waveguide as it happens in abrupt tapers.

In order to investigate the performance of tapered MMIs with an MM input and an SM output, we first discuss the design methodology. For any MMI structure, the input field profile at $z = 0$ can be written as a linear combination of the MM waveguide propagating modes,

$$\Phi(x, y, z = 0) = \sum_{m=0}^{M} c_m \phi_m(x, y), \tag{1}$$

where, c_m is the excitation coefficient calculated as the overlap integral of the input field (Φ) and the mth mode (ϕ_m), and $M + 1$ is the total number of supported guided modes. The field profile at $z = L$ can be written as

$$\Phi(x, y, z = L) = \sum_{m=0}^{M} c_m \phi_m(x, y) \mathrm{e}^{\mathrm{j}\varphi_m L}. \tag{2}$$

The accumulated phase of the mth mode is given as

$$\varphi_m(z) = \int_0^z n_{\mathrm{eff},m}(z') k_0 \, \mathrm{d}z', \tag{3}$$

where $k_0 = 2\pi/\lambda_0$ and $n_{\text{eff},m}$ is the effective index of the mth mode, which is a function of the MMI width at z. In order to have a single image at $z = L$ in the case of a symmetric excitation we must have

$$\Delta\varphi_2(L) = \varphi_0(L) - \varphi_2(L) = 2\pi. \quad (4)$$

Note that no odd modes are excited in the case of a symmetric excitation, which is the case for the tapered 1 × 1 MMI presented. As shown in figure 3(c), we calculate $n_{\text{eff},m}$ at $\lambda_0 = 1.55$ μm for the first two even modes in silicon-on-insulator-based devices from the finite element modeling (Rsoft FemSIM) of the waveguide structure cross-section shown in figure 1 inset. For the proof of concept, we assume an MM $t_1 = 2$ μm wide input silicon waveguide and an SM $t_2 = 0.5$ μm wide output silicon waveguide. The thickness of the silicon layer is 0.25 μm.

The input polarization is assumed to be TE. We have chosen the waveguide structure shown in the inset of figure 1 since it is a common SOI-based platform for silicon-based integrated photonic circuits [8, 9]. However, such a structure is polarization dependent because of the small core thickness and the large core/cladding index contrast [10]. However, such polarization dependence is not an inherent property of the tapered MMI device, and polarization-insensitive waveguide structures [11] can be used for polarization-independent mode conversion. It has been shown that the performance of MMIs implemented on the basis of such waveguide structures is polarization insensitive [11].

Since the input fundamental mode should be tapered down to $r = t_2/t_1$ of its original width, we should have $w_2/w_1 = r = 1/4$. Therefore, knowing the input and output waveguide widths and the MMI input width, we can find the MMI length, L, using equation (4) for any taper profile. We consider two tapering profiles, linear tapering and parabolic tapering, described as $w(z) = w_2 + (w_1 - w_2)(L - z)^2/L^2$. Using equations (3) and (4) and $n_{\text{eff},0}$ and $n_{\text{eff},2}$ values (figure 1(c)), we can calculate MMI length (L) required for onefold imaging under symmetric excitation. Figure 1(d) shows the variations of L versus w_1 for $w_2/w_1 = 1/4$ for both linear and parabolic tapering. Note that once the input and output widths are set, the MMI length and the tapering angle are derived from equation (4). Therefore, the tapering angle is not an independent design parameter.

3. Simulation results and discussion

Beam propagation simulations (Rsoft BEAMPROP) have been commonly used to characterize MMI-based devices [1, 5, 7]. Figures 2(a) and (b) show how a fundamental mode and a second-order mode, respectively, propagate in the tapered MMI structure and excite the SM output waveguide. As depicted in figure 2(a), this process is very efficient in the case of the fundamental mode, where the tapered MMI structure acts similarly to a conventional adiabatic MM to SM waveguide taper. In the case of the second-order mode input (figure 2(b)) some of the strong high order modes excited inside the MMIs are not supported at the narrowed output width of the tapered MMI. However, the SM

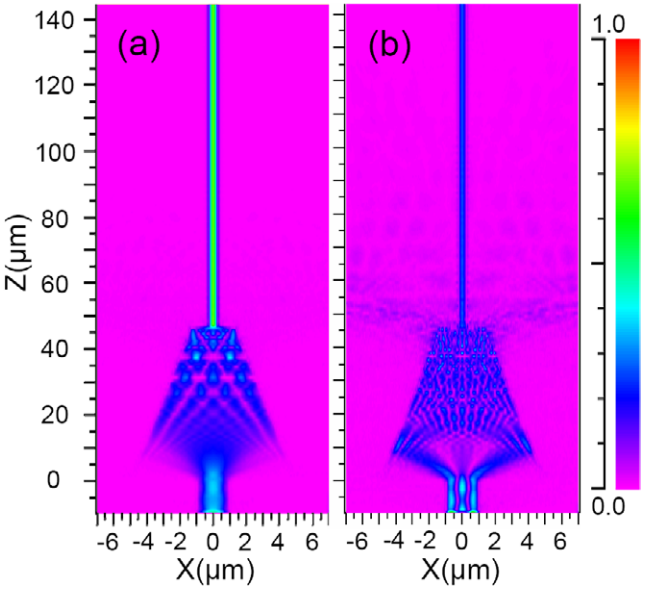

Figure 2. XZ field profile (E_x), BPM simulations of a linearly tapered 1 × 1 MMI coupler, $w_1 = 10$ μm, $w_2 = 2.5$ μm, $t_1 = 2$ μm, $t_2 = 0.5$ μm and $L = 46.4$ μm. Consider input excitations E_0 and E_2, which are the zeroth-order and second-order modes of the input waveguide (width = $t_1 = 2$ μm), respectively. E_0 and E_2 have the same power in our simulations. The tapered 1 × 1 MMI is excited by E_0 and E_2 in (a) and (b), respectively. (a) and (b) show $A_{00} = 0.996$ and $A_{20} = 0.255$, respectively.

output waveguide still receives a considerable excitation. An important observation is that the onefold image of the input forms at slightly different distances in figures 2(a) and (b). In figure 2(b), the onefold image formation plane is 0.1 μm closer to the input. This defocus effect is due to the relatively smaller n_{eff} values of the high order modes, compared to the values required for ideal self-imaging.

Figure 4 shows the variations of transmission coefficients (A_{m0}) versus the input MMI width (w_1) for the fundamental, second-order, and fourth-order mode inputs in both the linearly and parabolically tapered MMIs. In the case of the fundamental mode transmission (A_{00}), the linearly tapered structure efficiency remains above 98.5% in all cases. The parabolically tapered structure is less efficient, which can (especially for longer devices) be attributed to the increased radiation of high order modes out of the narrowed output of the MMI. In the case of A_{20}, the conversion efficiency depends on the output width of the MMI structure which is more prominent at smaller widths. A_{20} conversion also depends on the defocus effect, which is more prominent for longer (or equivalently wider) devices. Thus, A_{20} is slightly lower at both large and small widths for both linearly and parabolically tapered MMIs. The defocus effect is less effective in parabolically tapered MMIs due to their shorter lengths and A_{40} is considerably larger for the parabolic taper compared to the linear taper. The A_{20} curves for the linearly and parabolically tapered MMIs intersect at around $w_1 = 6$ and 10 μm. This discrepancy is due to the finite resolution and limited capability of the beam propagation simulations for capturing fast varying field profiles and relatively large angle beam direction changes for small w_1 values. Such behavior is not likely to be physically meaningful.

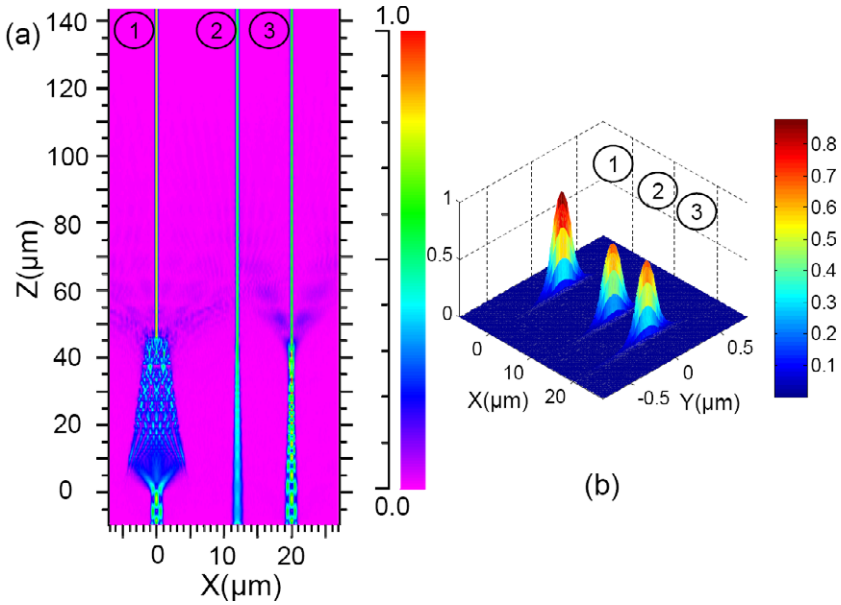

Figure 3. (a) and (b) show the XZ and XY field profiles (E_x), respectively. Device 1 is a linearly tapered 1×1 MMI ($w_1 = 10\ \mu$m, $w_2 = 2.5\ \mu$m, $t_1 = 2\ \mu$m, $t_2 = 0.5\ \mu$m and $L = 46.4\ \mu$m). Devices 2 and 3 are identical conventional MM to SM adiabatic tapers with input width $t_1 = 2\ \mu$m, output width $t_2 = 0.5\ \mu$m, and taper length $L = 46.4\ \mu$m. Consider input excitations E_0 and E_2, which are the zeroth-order and second-order modes of the input waveguide (width $t_1 = 2\ \mu$m), respectively. E_0 and E_2 have the same power in our simulations. Devices 1 and 3 are excited with both E_0 and E_2. Device 2 is excited only by E_0.

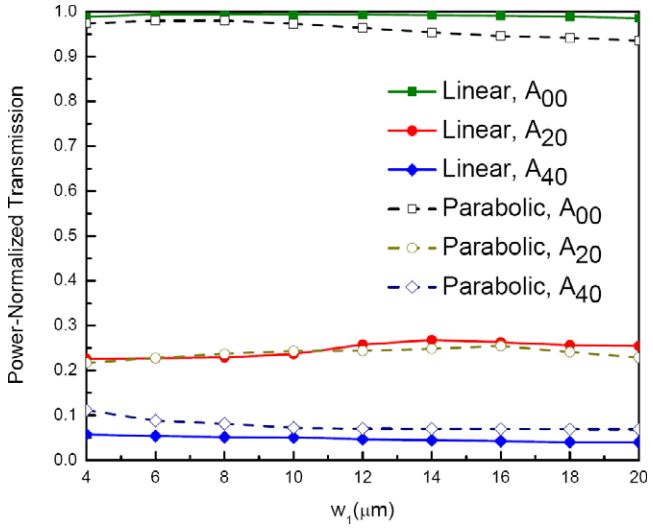

Figure 4. Variations of A_{m0} versus the input MMI width (W_1) for $t_1 = 2\ \mu$m, $t_2 = 0.5\ \mu$m. To calculate A_{m0} values, the output SM waveguide field amplitude is normalized to the output field amplitude of a conventional MM (width $= 2\ \mu$m) to SM (width $= 0.5\ \mu$m) adiabatic taper excited by the fundamental mode of the same input power.

As demonstrated in figure 4, if the input excitation contains both zeroth-order and the second-order modes of the same power, the field amplitude in the SM output can be 25% higher compared to that for an adiabatic taper of the same input and output waveguide widths, as depicted in figures 3(a) and (b). This results in over 55% increase in the output power. To achieve such efficiency, the zeroth-order and second-order input excitation in the SM output waveguide should be in phase. This phase matching condition is required for all mode converter/combiners [12, 6], where all modes have the same frequency, such as in exciting an MM planar waveguide using an MM fiber that was originally excited using a single-wavelength end-fire. However, if the modes are at slightly different wavelengths, such as the transverse modes of a diode laser [13], the SM output waveguide contains fundamental modes of different wavelengths, and the relative phase is not important.

4. Conclusion

We presented the first tapering scheme capable of near 100% transmission of the input fundamental mode, as well as mode conversion for input high order modes. When directly excited by diode lasers, the tapered MMI coupler presented can directly convert the fundamental mode and the second-order transverse mode of different wavelengths into the fundamental mode signals of an SM waveguide. Unlike the previously presented MMI-based mode converters [6], our MMI-based mode converter consists of a single-stage MMI. Therefore, the results can be also implemented in optical fibers for MM fiber to SM fiber coupling. All fiber MMI-based components, such as band-pass filters and refractometer sensors, have been theoretically and experimentally demonstrated [14].

Acknowledgment

This research is supported by the multi-disciplinary university research initiative (MURI) program through the AFOSR, contract # FA 9550-08-1-0394.

References

[1] Van Vaalen M and Smit M K 1988 *Fiber Integr. Opt.* **7** 235–9
[2] Baets R and Lagasse P E 1982 *Appl. Opt.* **21** 1972–8
[3] Yang L, Yang B, Sheng Z, Wang J, Dai D and He S 2008 *Appl. Phys. Lett.* **93** 203304
[4] Sahu P P 2008 *IEEE Photon. Technol. Lett.* **20** 638–40
[5] Dai D and He S 2008 *Appl. Opt.* **47** 38–44
[6] Leuthold J, Eckner J, Gamper E, Besse P and Melchior H 1998 *J. Lightwave Technol.* **16** 1228
[7] Miura T and Koyama F 2004 *Japan. J. Appl. Phys.* **43** L21
[8] Sridaran S and Bhave S A 2010 *Opt. Express* **18** 3850–7
[9] Sherwood-Droz N, Gondarenko A and Lipson M 2010 *Opt. Express* **18** 5785–90
[10] Vlasov Y and McNab S 2004 *Opt. Express* **12** 1622–31
[11] Sahu P P 2009 *Appl. Opt.* **48** 206–11
[12] Hermansson B, Yevick D and Danielsen P 1983 *IEEE J. Quantum Electron.* **19** 1246–51
[13] Eichhorn M, Rattunde M, Schmitz J, Kaufel G and Wagner J 2006 *J. Appl. Phys.* **99** 53105
[14] Mohammed W S, Smith P W E and Gu X 2006 *Opt. Lett.* **31** 2547–9